Determination of the phase of the diffracted field in the optical domain application to the reconstruction of surface profiles

Nathalie Destouches, Charles-Antoine Guérin, Michel Lequime, Hugues Giovannini

Determination of the phase of the diffracted field in the optical domain Application to the reconstruction of surface profiles

Nathalie Destouches, Charles-Antoine Guérin, Michel Lequime, Hugues Giovannini

1. Introduction

Diffraction is known to be a powerful method for the non-destructive and remote characterisation of targets. Indeed, measuring both amplitude and phase of the field diffracted by an object, gives precious information on its optogeometrical parameters such as its permittivity distribution or its shape. This technique is used, for example, in the radiofrequency domain to solve deterministic problems like the reconstruction of surface profiles or embedded objects [1]. In principle this method can be applied to any range of frequencies, depending on the size of the target. However, as an interferometric apparatus is required, determining the phase of the field in the optical domain is a difficult task. For this reason, most efforts have been devoted to the study of the diffracted intensity pattern. Although this information gives access to the second order (spectral density) statistical properties of the diffracting structure [2], the inverse deterministic problem when not using an optimisation method [3,4] requires phase measurements of the diffracted field.

The problem of detecting the phase of the field diffracted by an object has been addressed for different kind of applications. For example for chemical sensing applications that require the detection of small variations of permittivity, interferometric configurations have been proposed in order to measure the phase of the reflected beam near the electromagnetic resonances [5,6]. To separate

surface contribution and volume contribution to electromagnetic scattering, angle-resolved ellipsometric scatterometers have been developed [7,8]. In this case the polarimetric phase of the scattered field is measured. An experimental configuration [9] has recently been proposed to directly measure both amplitude and phase in a scanning near-field optical microscope [10]. The underlying principle is interference between a probe beam and a reference beam. However, extending this technique to far-field measurements is not straightforward. Indeed, in this case, accurate thermal and mechanical stabilisation is needed.

In this paper we present an experimental set-up which gives access, within the validity of Kirchhoff approximation, to the phase of the diffracted field in the incidence plane. The crucial advantage of our solution is its insensitivity to mechanical drifts or thermal fluctuations. We show that our technique can be used for reconstructing profiles of rough surfaces with a straight inversion of the experimental data i.e. without using any optimisation method. We illustrate this result by considering the particular case of periodic surfaces.

2. Principle of measurement

The principle of phase measurement of the field diffracted from a rough interface between two homogeneous media lies in the coherent mixing of two beams coming from the same laser source which overlap on the sample surface. The incidence angles of the two beams can be chosen independently as well as the observation direction of the scattered field. In a given direction, this scattered field results from the interference between the speckle patterns produced by the two incident beams. The phase information is measured by means of a synthetic heterodyne detection scheme. A photodetector rotating around the sample permits one to record the angular variations of the phase in the incidence plane. The phase is measured with respect to a reference signal given by a fixed detector. Light from a helium–neon laser ($\lambda = 633$ nm) is divided into two beams with the use of a beam splitter. The beams form the two arms of the interferometer (see Fig. 1). Light in one arm is coupled in a polarisation-maintaining optical fibre. The end of the fibre can rotate around the sample and the collimated output beam illuminates the sample. The other beam, which lies in the same plane as the former, passes through an electro-optic phase modulator (EOPM). The two beams of the interferometer are superimposed on the surface of the sample. Introducing an optical path delay allows one to set the optical path difference between the two arms of the interferometer to a value which is smaller than the coherence length of the source. The direction of polarisation of the incident light can be switched from TE to TM by rotating simultaneously the polariser, the EOPM and the optical axis of the fibre. An optical density is used to vary the intensity balance between the two beams overlapping on the sample surface. Rotating the sample around a vertical axis can vary the incidence angles of the two incident beams.

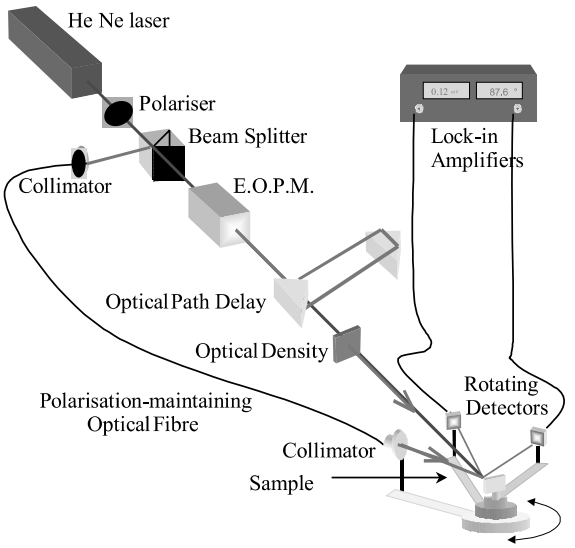

Fig. 1. Schematic of the experimental set-up. The detectors, the optical fibre and the grating can rotate around the same vertical axis.

A saw-tooth voltage modulation whose amplitude corresponds to a 2π phase shift is applied to the EOPM. Thus the interference signals obtained in all directions of space have a sine shape in time. In direction θ the scattered intensity can be written as:

$$I(\theta) = I_1(\theta, i_1) + I_2(\theta, i_2) + 2\sqrt{I_1(\theta, i_1) I_2(\theta, i_2)} \times \cos[\varphi(\theta, i_1) - \varphi(\theta, i_2) + \phi_0(t) + \Delta\xi], \quad (1)$$

where i_1 and i_2 are the incidence angles of beams 1 and 2, respectively. $\varphi(\theta, i_1)$ and $\varphi(\theta, i_2)$ are the phase shifts of the respective beams resulting from scattering from the surface sample in direction θ. $\phi_0(t)$ is the saw-tooth signal generated by the EOPM. The optical density is chosen in order to maximise the modulation amplitude of the interference signal recorded on the reference detector. Phase difference $\Delta\xi$ corresponds to the phase delay between the two incident beams, accumulated from the beam splitter to the sample surface. Obviously, any mechanical drift and any thermal fluctuation in the set-up, which affects the optical path delays of the two incident beams, causes $\Delta\xi$ to vary, making the measurement of $I(\theta)$ highly unstable. In order to avoid any complex stabilisation procedure, we propose a configuration with two measurement channels. The two outputs are processed to form a signal which is independent of $\Delta\xi$.

The two photodetectors placed in scattering directions θ and θ', are connected to a lock-in amplifier working in the phase detection mode. The measured phase ϕ is given by:

$$\phi = \varphi(\theta, i_1) - \varphi(\theta, i_2) - \varphi(\theta', i_1) + \varphi(\theta', i_2) \quad (2)$$

which is independent of $\Delta\xi$ and thereby insensitive to instabilities in the set-up. Away from plasmon anomalies [11], when working at nearly normal incidence, for small emergence angles and within the domain of application of Kirchhoff approximation (for theoretical developments see Section 3) ϕ can be written as follows (φ can be written a function of σ, σ', σ_1 and σ_2):

$$\phi = \varphi(\sigma - \sigma_1) - \varphi(\sigma - \sigma_2) - \varphi(\sigma' - \sigma_1) + \varphi(\sigma' - \sigma_2), \quad (3)$$

where $\sigma = (2\pi/\lambda)\sin\theta$, $\sigma' = (2\pi/\lambda)\sin\theta$, $\sigma_1 = (2\pi/\lambda)\sin i_1$ and $\sigma_2 = (2\pi/\lambda)\sin i_2$.

For θ' fixed and varying angle θ, if i_1 and i_2 are such as $\sigma_2 - \sigma_1 = \Delta\sigma$ the term ϕ_n given by:

$$\phi_n = \varphi(n\Delta\sigma) - \varphi[(n-1)\Delta\sigma] - \varphi(C\Delta\sigma) + \varphi[(C-1)\Delta\sigma], \quad (4)$$

where C is such as $\sigma' - \sigma_1 = C\Delta\sigma$, $\sigma_2 - \sigma_1 = \Delta\sigma$ and $\sigma - \sigma_1 = n\Delta\sigma$, can be calculated for all $n \in [-N/2; N/2]$. The discrete integration of phase terms ϕ_n permits one to determine the phase shift $\varphi_n = \varphi(n\Delta\sigma)$ corresponding to a scattering angle $\theta_n = \arcsin((\lambda/2\pi)n\Delta\sigma)$, to within a linear drift. However, as we will see, this drift has no influence on the reconstruction. Thus we can obtain the phase of the diffracted field at angles θ_n, the angular sampling rate being arbitrarily small.

When the sample is illuminated by only one incident beam, the set-up is equivalent to a classical angle-resolved scatterometer. For a fixed angle of incidence i_1, the intensity can be measured as a function of θ (of σ) and the complex amplitudes of the optical waves scattered in the incidence plane can be determined.

3. Profile reconstruction

Our set-up gives access to the value of the complex amplitude of the diffracted field in the incidence plane. We have applied our method of measurement to the problem of profile reconstruction. For the sake of simplicity, experiments have been performed with two metallic gratings. The samples are aluminium ruled gratings with 150 grooves/mm by Jobin-Yvon and with a grating height $h < 200$ nm. With these characteristics the grooves are shallow enough to ensure the validity of Kirchhoff approximation. Notice that, in normal incidence, 21 orders are diffracted from the gratings at wavelength $\lambda = 0.633$ μm. Detectors are silicon photodiodes working in photovoltaic regime placed in order to intercept the diffracted orders of interest. Measurements have been made by varying θ (and then σ) in all diffracted orders with $\Delta\sigma = (2\pi)/d$ (see Eq. (4)) where d is the grating period. Incidence angles i_1 and i_2 angles are chosen in order to avoid plasmon resonances that can occur with metallic surfaces illuminated in TM polarisation. This can be checked by measuring beforehand the reflectivity of the grating as a function of the angle of incidence.

For the reconstruction of the profile from the scattered field, the physical optics (Kirchhoff) approximation has been used. The latter is known to

be valid at non-grazing incidences for surfaces that are "smooth" on the scale of the wavelength. This goes for surfaces whose radius of curvature is much greater than the wavelength (see e.g. Ref. [12] for a thorough discussion). For 1D perfectly conducting surfaces, if θ designates the scattering angle and i designates the incidence angle, the scattered amplitude in the Kirchhoff approximation can be written as:

$$S(\theta,i,f) = A_0(\theta,i)\frac{1}{2\pi}\int \exp[-\mathrm{j}(\sigma-\sigma_i)x - \mathrm{j}(\beta-\beta_i)f(x)]\,\mathrm{d}x, \quad (5)$$

where $\beta = (2\pi/\lambda)\cos\theta$, $\beta_i = (2\pi/\lambda)\cos i$ and A_0 is an optical factor depending on the polarisation.

Note that in the case of an echelette grating, the Kirchhoff approximation is not valid near the edges. However, since the grating period is much greater than the wavelength, we will neglect the edge diffraction. We will also assume the grooves to be too shallow to cause multiscattering phenomena. These two assumptions ensure the validity of the Kirchhoff approximation. Working at normal incidence and small emergence angles, one has $\cos i \approx \cos\theta \approx 1$, so that the Kirchhoff approximation is reduced to the Fourier transform of the exponentiated profile (Fraunhofer approximation):

$$S(\theta,i) \propto \frac{1}{2\pi}\int \exp\left[-\mathrm{j}(\sigma-\sigma_i)x - \mathrm{j}\frac{4\pi}{\lambda}f(x)\right]\mathrm{d}x. \quad (6)$$

Then

$$\exp\left[-\mathrm{j}\frac{4\pi}{\lambda}(f(x))\right] = F\,T^{-1}[S(\theta,i)]. \quad (7)$$

Thus, the profile inversion is obtained from a bare inverse Fourier transform of the diffracted far field. Note that Eq. (7) shows that the modulus of the inverse Fourier transform of $S(\theta,i)$ is equal to 1. This can be used to verify the accuracy of the experimental results. In principle there exist a more accurate procedure for profile retrieval for the Kirchhoff approximation [13], but we found it hardly tractable at the experimental level since it requires simultaneous variations of the incidence and emergence angles.

4. Numerical study

4.1. Validity of the approximation used

In order to check numerically the validity of the approximation used, we have compared different initial profiles to those reconstructed from Eq. (7). For the comparison, the complex amplitudes $S(\theta,i)$ have been calculated with a rigorous method based on the differential formalism [14,15]. The comparison has been drawn for an echelette profile and for a sinusoidal one. For the echelette profile the blaze angle α was chosen as $\alpha = 3°$ and the depth as $h = 348$ nm. The depth of the sinusoidal profile is $h = 300$ nm. Fig. 2(a) shows the results obtained for these two particular cases. One

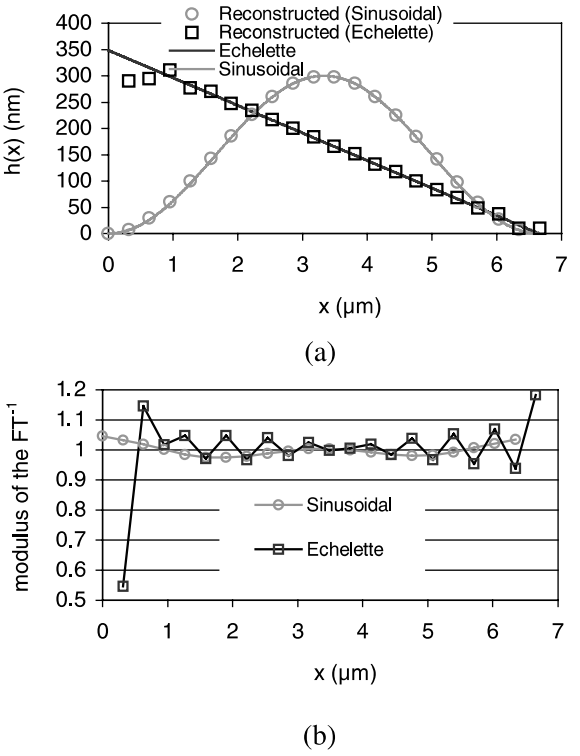

Fig. 2. (a) Comparison between the grating profiles and the reconstructed profiles: $h = 300$ nm for the sine profile and $h = 348$ nm and $\alpha = 3°$ for the echelette profile, $d = 6.67$ μm (150 grooves/mm), normal incidence. For the numerical calculations of the amplitudes of the diffracted orders, the refractive index of the grating was set to $n = 1.2 + 4.5\mathrm{j}$ which is close to that of aluminium. (b) Modulus of the Fourier transform as a function of the same abscissa x.

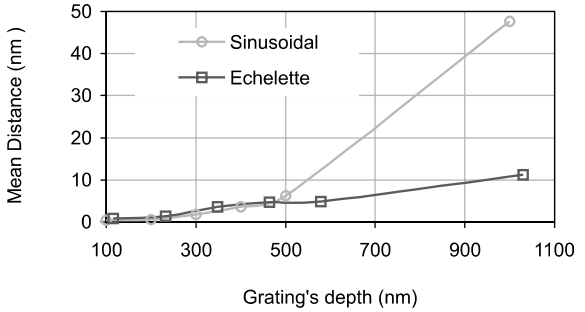

Fig. 3. Numerical simulation: root mean square distance between the grating profile and the reconstructed profile as a function of grating's depth h. Note that for the echelette grating the apex angle remains equal to 90° and the blaze angle increases with the grating's depth.

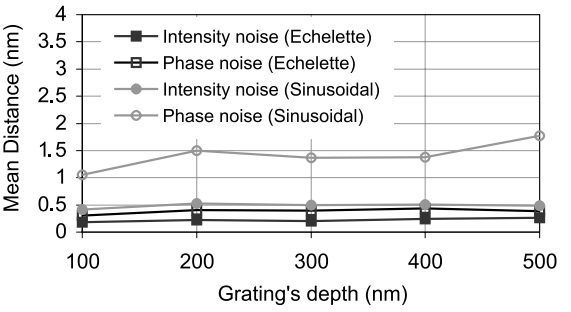

Fig. 4. Influence of the errors of measurement: The parameters of the gratings and the values of $S(\theta, i)$ determined by a rigorous method of computation are the same as those of Fig. 6.

can see that with this value of h both profiles can be determined accurately. Nevertheless, as expected (see Section 3), a slight disagreement is obtained near the edges of the echelette profile. One can notice (Fig. 2(b)) that a disagreement between the reconstructed profile and the initial one leads the modulus of the inverse Fourier transform to be different from unity. Thus, studying this modulus gives precious information about the accuracy of the result. Fig. 3 gives the mean distance $((1/N)\sum |h_{\mathrm{ini}}(x_i) - h_{\mathrm{rec}}(x_i)|)$ between the initial profile (echelette or sinusoidal) and the one determined from Eq. (7), as a function of the grating's depth. One can see that an error less than 3 nm is obtained for values of $h < 300$ nm.

4.2. Influence of the errors of measurement

We have also checked the stability of the reconstruction method of the inversion in relation to the experimental noise. We have successively introduced, on the numerical data, a 5° phase random noise and a 5% random noise on the modulus of $S(\theta, i)$. Fig. 4 shows the root mean square difference between the initial profile (echelette or sinusoidal) and the one determined from Eq. (7). One can see that such noises lead to a mean error smaller than 2 nm on the surface profile. This result shows the robustness of the inversion method used.

5. Experimental results

The arrangement of the optical experiment is shown in Fig. 5. Fig. 6 gives the comparison of the profiles as measured by atomic force microscopy (AFM) and the profiles obtained after reconstruction. AFM measurements of the surfaces have been performed with a contact tip on a 50 μm^2 area, with a sampling interval of 166 nm. The AFM curves drawn in Fig. 6 are the mean profiles along the invariance direction. In the optical experiment the beam size was 6 mm^2. For both gratings the

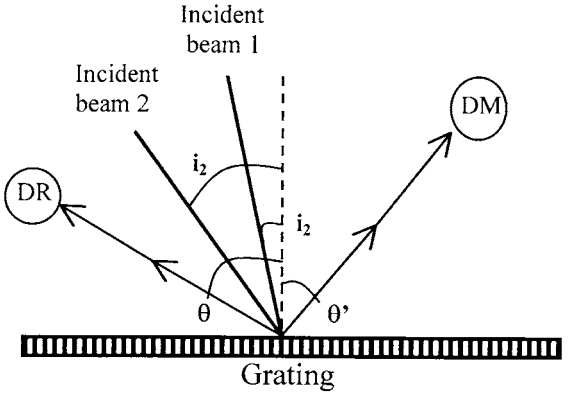

Fig. 5. Experimental arrangement: DR is the (fixed) reference detector ($\theta = 24.02°$). The second detector (DM) is rotated in order to intercept the diffracted orders of interest. Incidence angles i_1 and i_2 are chosen so that orders diffracted by the grating are superimposed ($i_1 = 1.57°$, $i_2 = 7.02°$). For convenience we do not represent all diffracted orders.

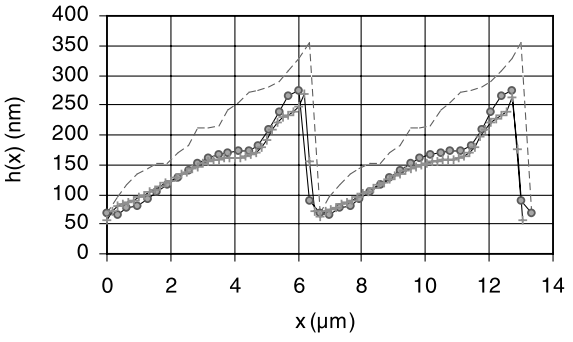

(a)

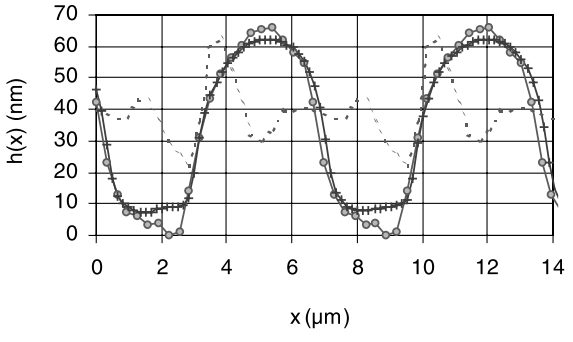

(b)

Fig. 6. Experimental results: profile of the diffraction grating along two periods. The results obtained from phase measurements (circles) are compared to those given by AFM measurement (cross). Dotted line is the result of the reconstruction when the phase of $S(\theta, i)$ is set to a random value. (a) Echelette grating and (b) sinusoidal grating.

optical experiment was performed by rotating one detector in order to successively intercept all the diffracted orders. This means that $n \in [-10, 10]$ (see Eq. (4)). The grating's height is about 200 nm for the echelette grating and the defects of ruling are clearly visible. The mean distance between the result obtained by AFM and the reconstructed profile is less than 7 nm. The height of the sinusoidal profile is about 60 nm and the mean distance between curves is 2.5 nm. In the reconstruction procedure the gratings' profiles are assumed to be invariant within the beam area. The discrepancy between the AFM data and the reconstructed profiles can be attributed to the partial validity of this assumption. Note that the same results are

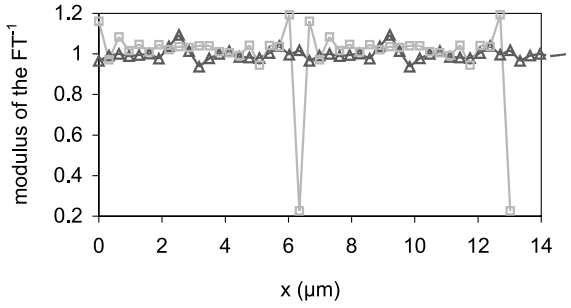

Fig. 7. Modulus of the Fourier transform of $S(\theta, i)$ experimentally obtained: Squares are relative to echelette profile and triangles are relative to sinusoidal profile.

obtained for TE and TM polarisations. This confirms the validity of the scalar approximation used.

To show the necessity of measuring the phase in reconstruction problems, the inversion has been performed by replacing the measured phases with a random phase (dotted lines in Fig. 6(a) and (b)). The profiles obtained this way do not have the same shape as the AFM-measured profiles. The necessity of measuring the phase is more clear in the case of a sinusoidal profile. For the echelette profile the reconstructed profile resembles however to an echelette profile, which is a generic phenomenon when efficiency in one order is very strong. Indeed, this implies a quasi-linear phase for the exponentiated profile. Fig. 7 gives the modulus of the Fourier transform (see Eq. (7)) of the experimental values of $S(\theta, i)$. Following the remark of Section 4 these results confirm the accuracy of the experimental data.

6. Conclusion

We have shown the possibility of measuring the phase of the diffracted field with an interferometric set-up insensitive to instabilities. The angular phase information, which is obtained from a small number of measurements, can be used for reconstructing grating profiles. The inversion method described can be generalised to the case of rough surfaces whose optogeometrical parameters are so that Kirchhoff approximation can be used. Dielectric surfaces may also be studied with a suitable theory.

References

[1] S. Bonnard, M. Saillard, P. Vincent, J. Opt. A 1 (1999) 566.
[2] J.M. Elson, J.P. Rahn, J.M. Bennet, Appl. Opt. 19 (1980) 669.
[3] A. Roger, D. Maystre, J. Opt. Soc. Am. 70 (12) (1980) 1483.
[4] A. Roger, M. Breidne, Opt. Commun. 35 (3) (1980) 299.
[5] S.G. Nelson, K.S. Johnston, S.S. Yee, Sensors Actuators B 35–36 (1996) 187.
[6] P.I. Nikitin, A.A. Beloglazov, V.E. Kocherin, M.V. Valeiko, T.I. Ksenevich, Sensors Actuators B 54 (1999) 43.
[7] C. Deumié, H. Giovannini, C. Amra, Appl. Opt. 35 (28) (1996) 5600.
[8] T.A. Germer, Phys. Rev. Lett. 85 (2000) 349.
[9] P.L. Phillips, J.C. Knight, J.M. Pottage, G. Kakarantzas, P.St.J. Russell, Appl. Phys. Lett. 76 (5) (2000) 541.
[10] D.W. Pohl, W. Denk, M. Lanz, Appl. Phys. Lett. 44 (1984) 651.
[11] M.C. Hutley, D. Maystre, Opt. Commun. 19 (3) (1976) 431.
[12] J.A. Ogilvy, Theory of Wave Scattering from Random Rough Surfaces, Adam Hilger, Boston, MA, 1991.
[13] R.J. Wombell, J.A. DeSanto, J. Opt. Soc. Am. A 8 (12) (1991) 1892.
[14] F. Montiel, M. Nevière, J. Opt. Soc. Am. A 11 (1991) 3241.
[15] L. Li, J. Opt. Soc. Am. A 13 (1991) 1024.